Supporting Information for

Capillary Force-Induced Au nanoparticle-Ag nanowire Single Hot Spot Platform for SERS Analysis

Pan Li,[a,b] Xiunan Yan,[a,b] Fei Zhou,[c] Liangbao Yang,[a,b*] Jinhuai Liu [a,b]

[a] Institute of Intelligent Machines, Chinese Academy of Sciences, Anhui, Hefei 230031, China

[b] Departmen t of Chemistry, University of Science & Technology of China, Anhui, Hefei 230026, China

[c] Institute of Solid State Physics, Chinese Academy of Sciences, Hefei 230031, China

*L.B.Y. (lbyang@iim.ac.cn). Fax: (+86)551-65592420

Contents

Section 1. Chemical materials and experimental setups

$AgNO_3$ (99+%), poly(vinyl pyrrolidone)(K-30), trisodium citrate and paraoxon were purchased from Sinopharm Chemical Reagent Co., Ltd. (China). Ethylene glycol (EG, anhydrous, 99.8%), p-aminothiophenol (p-ATP), rhodamine 6G (R6G), malachite green (MG), cysteine, and adenosine-5'-triphosphate were purchased from Sigma-Aldrich. Methamphetamine (MA) was purchased from the Academy of Military Medical Sciences (China). All chemicals used in this study were of analytical grade. $HAuCl_4 \cdot 3H_2O$ was obtained from Shanghai Chemical Co., Ltd. (China). All the solutions were prepared in double-distilled water.

Scanning electron microscopy (SEM) images were acquired using a field-emission scanning microscope (QUANTA 200FEG, FEI) at an accelerating voltage of 10 kV. UV-vis absorption spectra were recorded using a Shimadzu UV-2550 spectrophotometer (Japan). Transmission electron microscopy (TEM) images were recorded by a JEOL 2010 high resolution transmission electron microscope equipped with an Oxford INCA energy dispersive spectroscopy (EDS) system at an accelerating voltage of 200 kV.

Section 2. Synthesis and characterization of the Ag NWs and Au NPs

For the synthesis of Ag NWs:[1] 10 mL of EG was first refluxed in a three-necked round-bottom flask at 160°C for 2 h. Then, 5 mL of EG solution of $AgNO_3$ (0.1 M, 0.169 g) and 5 mL of EG solution of 0.222 g of poly (vinyl pyrrolidone) (PVP, K-30) were simultaneously injected into the refluxing solvent at a rate of 0.2 mL/min. Finally, this reaction mixture was heated at 160°C for 60 min. The NWs were separated from particles using centrifugation. In this case, the reaction mixture was cooled to room temperature, diluted with acetone (approximately 10 times by volume) and washed three times (centrifuged at 2,000 rpm for 20 min); diluted with ethyl alcohol (10 mL) and washed three times (centrifuged at 2,000 rpm for 20 min); and then diluted with water (10 mL) and washed three times (centrifuged at 2,000 rpm for 20 min). The synthesis resulted in single Ag NW with a diameter of 110 nm and an average length of 10 μm.

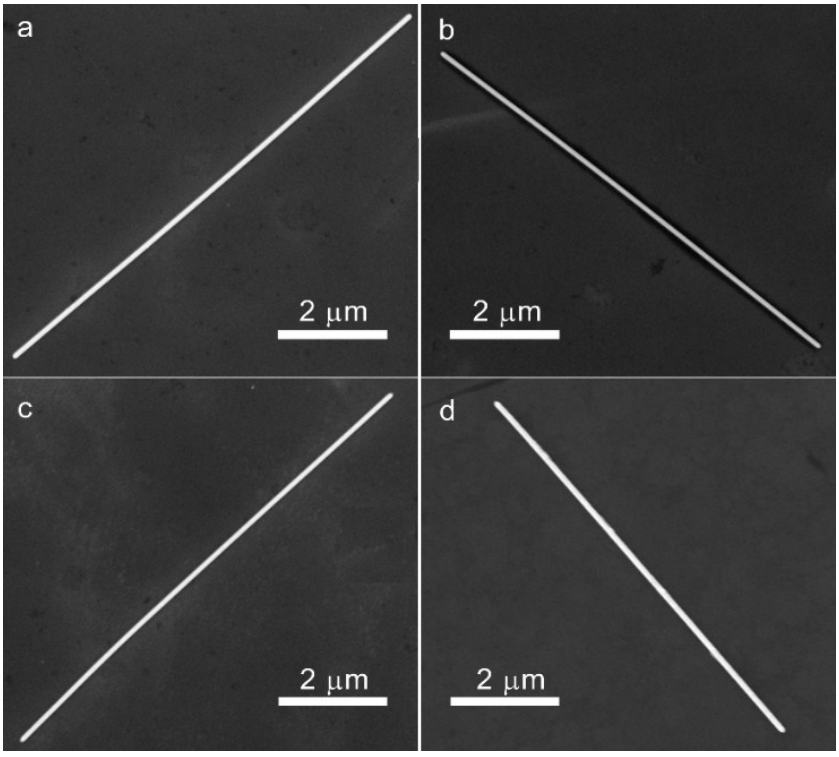

Fig. S1 SEM images of several single Ag NW (a-d) with a diameter of 110 nm and length of 10 μm**.**

Au NPs were prepared based on a classical method.[2] For the synthesis of Au NPs, 1 mL of $HAuCl_4$ (1%) aqueous solution was diluted with 90 mL of water and then boiled under vigorous stirring. Then, 1 mL of citrate (1%) aqueous solution was used as a reductant and quickly added. This solution was used as Au seeds (~50 nm) to prepare larger Au NPs. Au NPs with an average diameter of approximately 90 nm were obtained as follows: the mixed solution with 10 mL of Au seed solution, 0.4 mL of NH_2OH (25 mM) solution, 28.4 mL of water and 0.4 mL of citrate (1%) solution were vigorously stirred for 5 min. Then, 0.8 mL of $HAuCl_4$ (1%) aqueous solution was added, and the above solution was stirred for another 1 h.

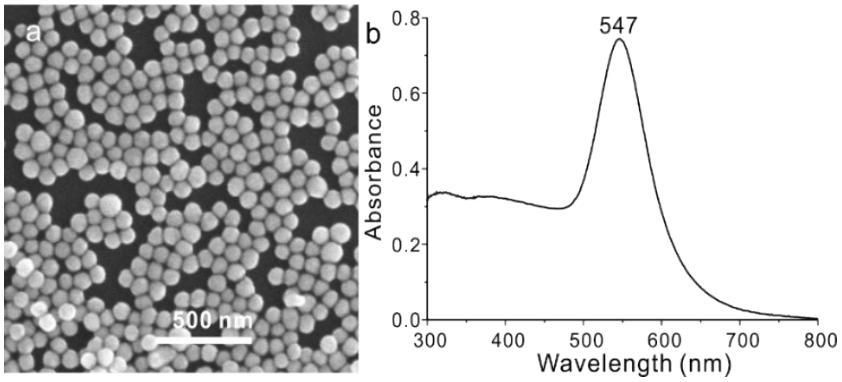

Fig. S2 (a) SEM images and (b) UV-Vis absorption of Au NPs with a diameter of approximately 90 nm.

Section 3. Mathematical model for assembled possibility of single hot spot structures

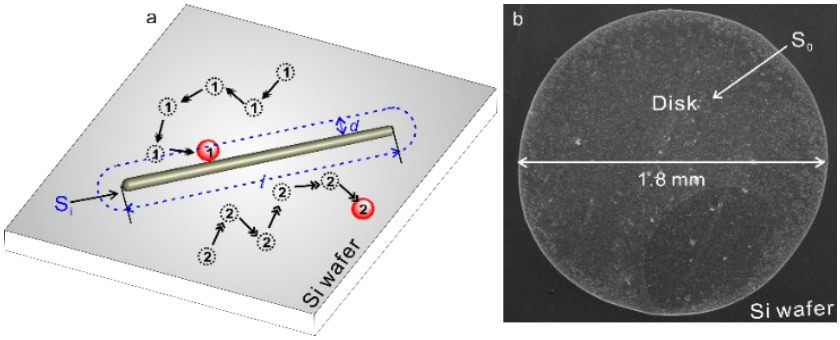

Fig. S3 (a) Schematic diagram of a proposed mechanism of how a single Au NP moves toward the surface of the NW, where S_i is the efficient area dominated by the capillary force around a single Ag NW; (b) the SEM image of Ag NW (1 μL) drop drying on the hydrophilic Si wafer, where the area disk is denoted by S_0 .

Under non-vacuum conditions, a liquid bridge between two granular media can be formed by spontaneous capillary condensation from the ambient vapor. In the free-liquid thermodynamic equilibrium approach, it is assumed that the two principal radii of an elongated concave meniscus are strictly related by the well-known Kelvin equation.[3, 4] Upon approach between two wet granular media, a sudden attractive force is exerted on the wet granular media; if

the two wet granular media approach further, the force increases linearly with decreasing distance. The maximum attractive interaction is reached immediately before contacting each other. In terms of the length of the liquid bridge, if no external perturbations are present, the elongated capillary will be disrupted at the capillary instability point.

Section 4. Assembly of single hot spot structure using spontaneous capillary force

In this report, the length (l) and diameter ($2R$) of the Ag NW are 10 μm and 110 nm, respectively, based on the SEM and TEM images. Here, for convenience, the cross section of the Ag NW is denoted by a circle, and the number (K) of Ag NWs in the synthesized 20 mL solution (without diluted) can be obtained by the following equation:

$$L = \frac{C_{AgNO_3} V_{AgNO_3} M_{Ag}}{\rho_{Ag} \pi R^2} (n_{AgNO_3} = n_{Ag^+}) \quad (1)$$

$$K = L / 10\mu m = 3.8 \times 10^{10}$$

During the assembly process, all the synthesized Ag NWs were diluted to 200 mL with water, and then, 1 μL of Ag NWs (k =1.9×10^5/μL) were dropped onto the Si wafer. After drying, the Au NPs were added on the Si wafer. The numbers (N) of Au NPs in 1 mL of solution were calculated with the following equation:

$$N = \frac{m_{Au}}{m_{AuNPs}} = \frac{C_{HAuCl_4} V_{HAuCl_4} M_{Au}}{\rho_{Au} V_{AuNPs}} = \frac{C_{HAuCl_4} V_{HAuCl_4} M_{Au}}{\rho_{Au} \frac{4}{3} \pi R^3} (n_{HAuCl_4} = n_{AuNPs})$$

$$= 5.9 \times 10^{12} / 100mL \quad (2)$$

$$= 5.9 \times 10^{10} / mL$$

Anything above 10 mL of Au NPs was removed as seeds for further growth. The number of Au NPs within the average diameter of 90 nm can then be calculated as $1.5 \times 10^9 / mL$. Following this calculation, 1 μL of Au colloids (1,000-fold dilution) containing 1.5×10^6 Au NPs was dropped onto the Si wafer to form the single hot spot structure.

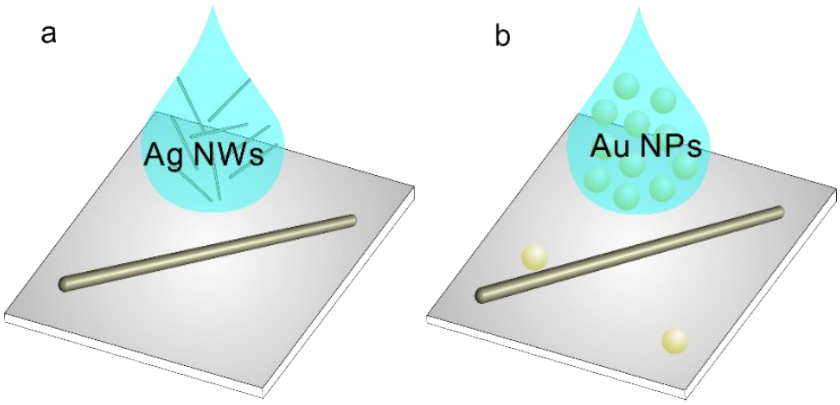

Fig.S4 (a) The deposition of Ag NWs on the Si wafer and (b) the assembly of Plasmon NW-NP structure by using the capillary force.

Section 5. Supplementary dark-field video

Video I shows the gradual adsorption of the Au NP toward the Ag NW, which indicates that spontaneous capillary imbibition can efficiently drive the Au NP toward the Ag NW to form single hot spot structure.

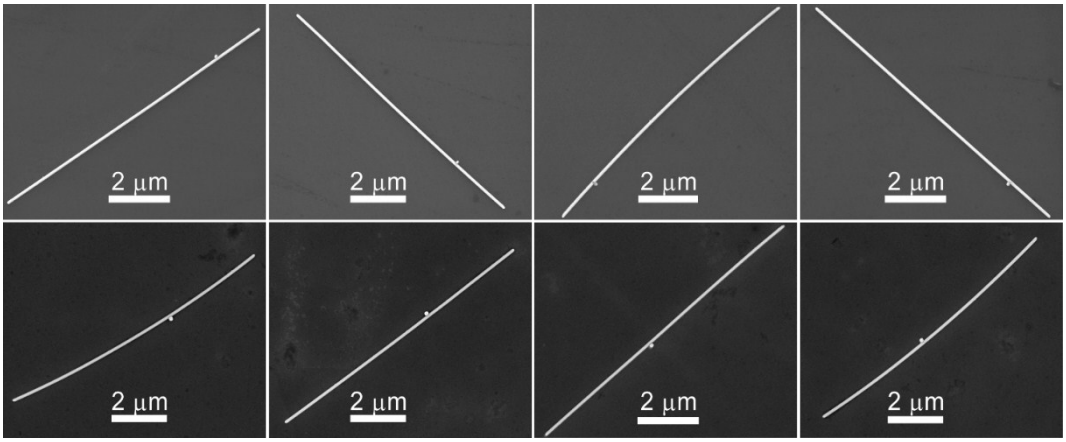

Fig. S5 SEM images of single hot spot structures.

Section 6. Characterization of the single hot spot structure

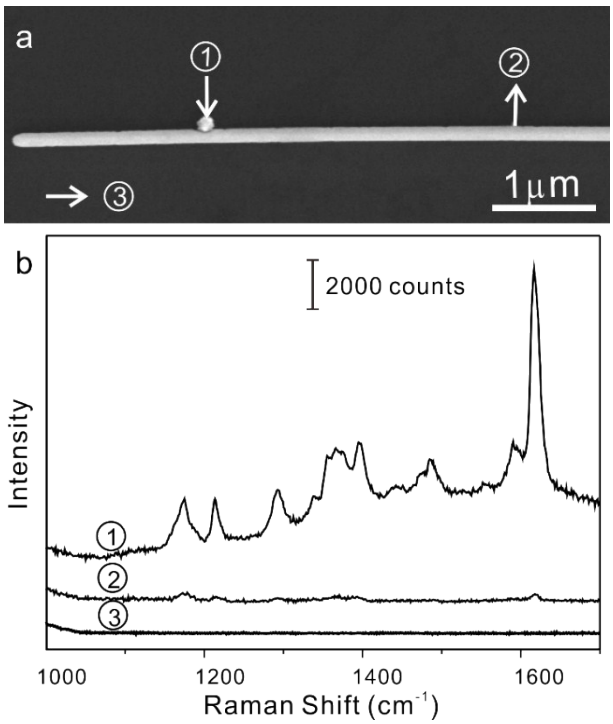

Fig. S6 (a) SEM image of the coupled Au NP-Ag NW single hot spot structure and (b) SERS spectra of malachite green (MG, 1 μM) for different positions of the single hot spot structure. All the SERS spectra were recorded with

an integration time of 1.8 s and a laser power of 2 mW under 633 nm laser excitation.

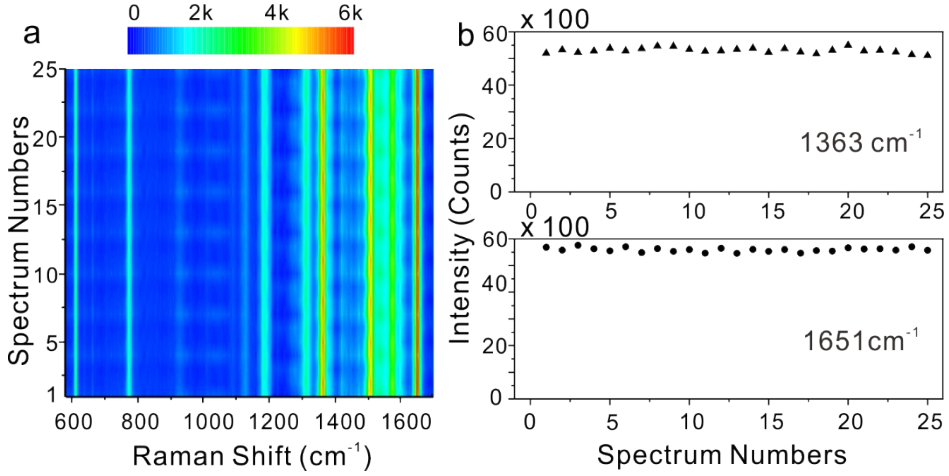

Fig. S7 (a) The 2D-SERS mapping of rhodamine 6G (R6G, 1 μM) and (b) the variation of SERS intensity at the Raman modes of 1363 and 1651 cm^{-1} collected from 25 random single hot spot substrates. All the SERS spectra were recorded with an integration time of 1.8 s and a laser power of 2 mW under 633 nm laser excitation.

Section 7. Supplementary theoretical and experimental analysis

Section 7.1 Calculation of the theoretical enhancement factor ($\left|E / E_0\right|^4 = EF$)

The structures are simulated by the finite-difference time-domain method. The geometric parameters of the NW and NP are measured by SEM and TEM. Perfect matched layer (PML) boundary conditions are adopted along x, y and z axes. The NW is placed along the x direction in the x-y plane, and the nano-sphere is also in the x-y plane with a gap of 1.5 nm to the NW. The incident light is injected along the z-axis with an electric field along the y-axis. The dielectric functions of silver and gold are obtained from Palik's data (Handbook of Optical Constants of Solids, Edited by Edward D. Palik, Institute for Physical Science and Technology, University of Maryland College Park, Maryland). The simulation mesh is 0.25 nm.

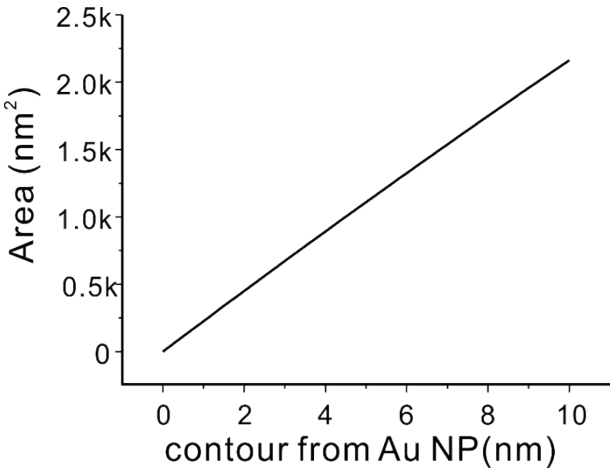

Fig. 8 Calculation of the hot area (*A*) that experienced significant E-field enhancement.

Section 7.2 Calculation of the number of molecules

In this report, the single hot spot area is considered the distance between the NP and NW, and a distance less than 10 nm is defined as the efficient enhancement area, called a single hot spot area (2,500 nm^2). The cross section of the Ag NW is denoted by a circle, and the numbers (*K*) of Ag NWs in the synthesized solution (without diluted) can be obtained with the following equation:

$$L = \frac{C_{AgNO_3} V_{AgNO_3} M_{Ag}}{\rho_{Ag} \pi R^2} (n_{AgNO_3} = n_{Ag^+}) \tag{3}$$

$$K = L / 10\mu m = 3.8 \times 10^{10}$$

Moreover, by adding the target molecules into the 1 mL of Ag NW sol containing 1.9 × 10^8 single Ag NWs (the synthesized Ag NW sol was diluted to 200 mL with ultrapure water), the density ρ of molecules on the single Ag NW substrate surface is estimated to be a monolayer[5] with a concentration of 1 *p*mol (1 *p*mol = 5 μL × 0.2 μM) dye molecules, such as MG or R6G (where S represents the superficial area of a single Ag NW defined as a cylinder):

$$\rho = \frac{C_{analyte} V_{analyte} N_A}{k S_{nanowire} / 200} = 1.95 molecules / nm^2 (S = 10^4 \pi R^2) \tag{4}$$

If all molecules have been adsorbed onto the Ag NWs (1 mL), the contact surface defined as the "hot spot area" experiencing the giant E-field with an area of 2,500 nm^2 can carry approximately 4.88 ×10^3 analyte molecules based on the above calculation.

Section 7.3 Calculation of the experimental enhancement factor (EF)

To gain a better understanding of the single hot spot formed between Au NP and Ag NW, we investigated the experimental EF. The EF for the single hot spot structure was estimated using the following equation:

$$EF = \frac{I_{SERS} / N_{Surf}}{I_{RS} / N_{Vol}} \tag{5}$$

where I_{RS} and I_{SERS} are the Raman intensity for an average number N_{Vol} of molecules in the scattering volume and the SERS intensity for an average number N_{Surf} of molecules adsorbed in the sub-monolayer range onto the metal surface in the same scattering volume, respectively.

Assuming that the excitation volume is a cylinder, the diameter d as determined by the following equation:

$$d = \frac{1.22\lambda_{laser}}{NA} = 0.85\mu m \tag{6}$$

I_{SERS} represents the SERS intensities at 1617 cm^{-1} collected from MG with a concentration of 1 pmol (1 pmol = 5 μL × 0.2 μM), and can be calculated to be approximately 4.88 $\times 10^3$ analyte molecules (N_{surf}) adsorbed onto the hot spot area (2,500 nm^2), which is approximately 6,120 counts; I_{RS} represents the SERS intensities at 1617 cm^{-1} collected from MG with a concentration of 0.2 μM (0.2 μmol = 1μL × 0.2 M) in the laser excitation volume on the Si wafer and can be calculated to be approximately 8.6× 10^{10} analyte molecules (N_{Vol}), which is approximately 161 counts. Herein, 1 μL of analyte solution on the Si wafer produced a deposition area of 1 mm in diameter. Assuming uniform distributions of all molecules on the Si wafer, there were an average of 8.6 × 10^{10} molecules (8.6 $\times 10^{10}$ = 0.2 μmol × 6 × 10^{23} molecules·mol^{-1}/π(500 μm)^2 /π(0.425 μm)^2) within the scope of the laser spot (0.85 μm in diameter). Consequently, the experimental EF for the MG molecules within the hot spot area can be calculated to be approximately 6.8 × 10^8.

Section 7.4 Effect of Au NPs position relative to Ag NW on the $|E/E_0|$ distribution

In the present calculations, single Au NP was randomly captured on the surface of the NW through spontaneous capillary imbibition. The positions of Au NPs interacting with Ag NW were not considered, so we next investigated how the position of the Au NP coupled with NW, such as its interactions with the tip and side as well as the center of the NW, affected the E-field enhancement. Generally, when surface plasmon polaritons (SPPs), the collective motion of free electrons, are excited in the plasmonic waveguides, they can be propagated at distances exceeding tens of micrometers in nanometer-width geometries, such as NWs or NP chains.[6] However, a uniform long metallic wire cannot couple to light because of the mismatch of the photon and wire plasmon dispersion relations. Alternatively, a metallic NP adjacent to a metallic wire can serve as an efficient nano-antenna, providing a means for coupling light into and out of the propagating wire plasmon, as well as providing localized giant E-field enhancement.[7, 8] Consequently, the presence of Au NPs excites the surface plasmon of the NW, which in turn

generates the SPP on the Ag NW and induces the large localized E-field at the gap between the NP and NW. Therefore, the theoretical $|E/E_0|$ distribution of the hot spot with respect to the center of the NW is compared with results obtained on the tip of the NW, which show good agreement. Namely, the position of the Au NP relative to the Ag NW has only a slight influence on the E-field distribution for the single hot spot structure.

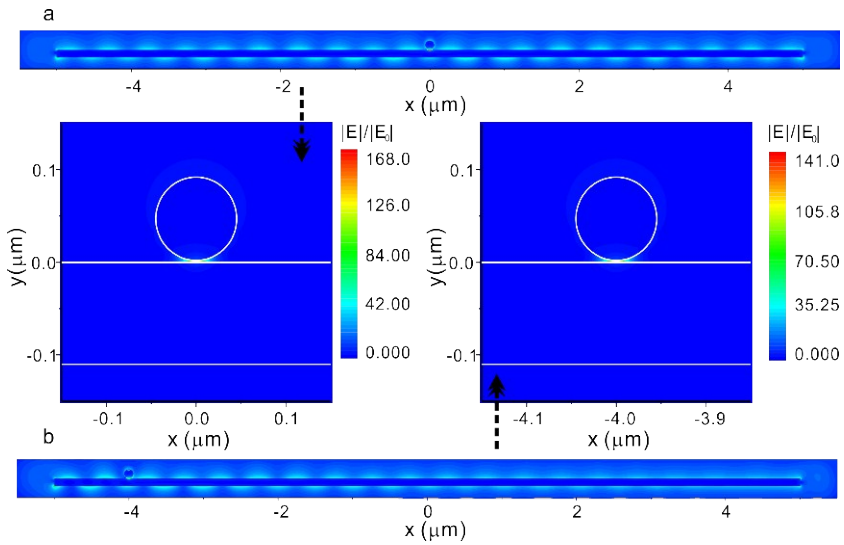

Fig. S9 Different E-field enhancement with 633 nm laser for different positions of the Au NP interacting with the NW: (a) at the center position of the NW and (b) at the tip position of the NW.

Section 7.5 Effect of two NPs coupled with NW separated with different distance on the $|E/E_0|$ distribution

Another important question concerns two NPs with different distances that are both coupled with the NW. Whether a single hot spot can always act as a representative hot spot structure and then provide similar E-field enhancement with excitation of the surface plasmon for the Ag NW coupled with two Au NPs. To this end, FDTD was used to simulate the two gap modes on a single NW. Although the uniform Ag NW cannot couple to light due to the mismatch of the photon and wire plasmon dispersion relations, if the symmetry of the Ag NW is gently broken over longer length scales, such as coupling with NP or surface defects, the Ag NW SPP can be excited and propagated. Thus, the coupled site will produce considerable E-field enhancement. In this report, when using the 633 nm laser, the SPP for the NW-NP structure is 500 nm. As two Au NPs separated with different distances have been coupled with the Ag NW, the propagative SPP will have interacted with each other; however, the localized E-field enhancement is larger than the interactive PSP. Therefore, for two Au NPs separated by 1.25, 1 and 2 μm, the E-field enhancement was 17×10^8, 4.4×10^8 and 3.2×10^8, respectively, with minor fluctuations for the SERS enhanced signals.

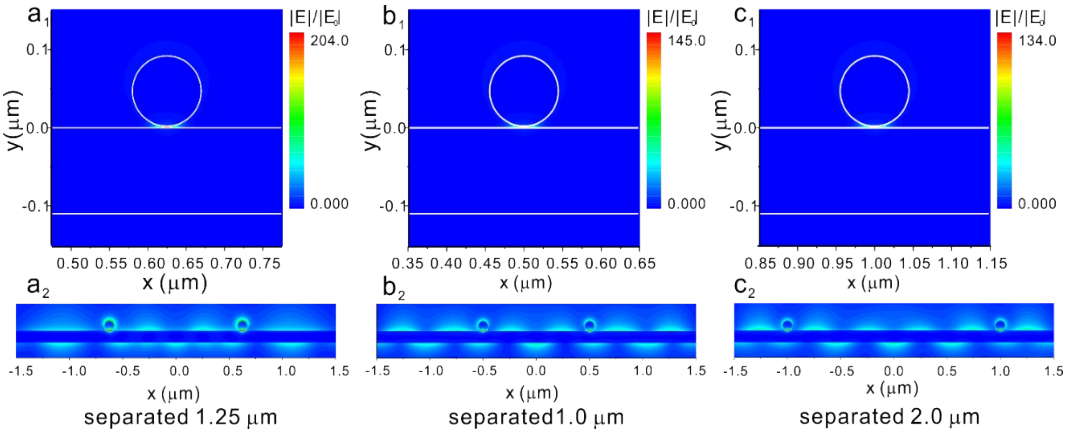

Fig. S10 Effect of two NPs coupled with Ag NWs and separated with different distances (a) 1.25 μm, (b) 1.0 μm and (c) 2.0 μm on EF distribution with 633 nm laser.

Section 8. Supplementary tip (AFM)-correlated Raman analysis

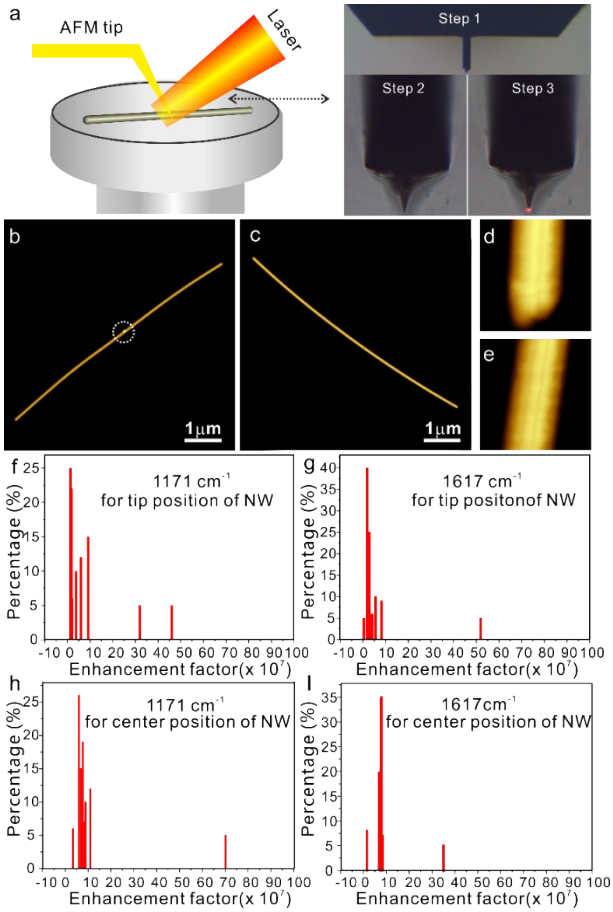

Fig. S11 The AFM-correlated single NW Raman analysis and SERS enhancement factor distributions. (a, b) The working principles of AFM-correlated Raman technique and corresponding corrective steps; (b-e) the representative

AFM images of single hot site structure and single Ag NW; and (f-i) the distribution diagrams of the measured EF at 1171 cm^{-1} and 1617 cm^{-1} (MG molecules) for AFM interacting with tip and center position of NW, respectively.

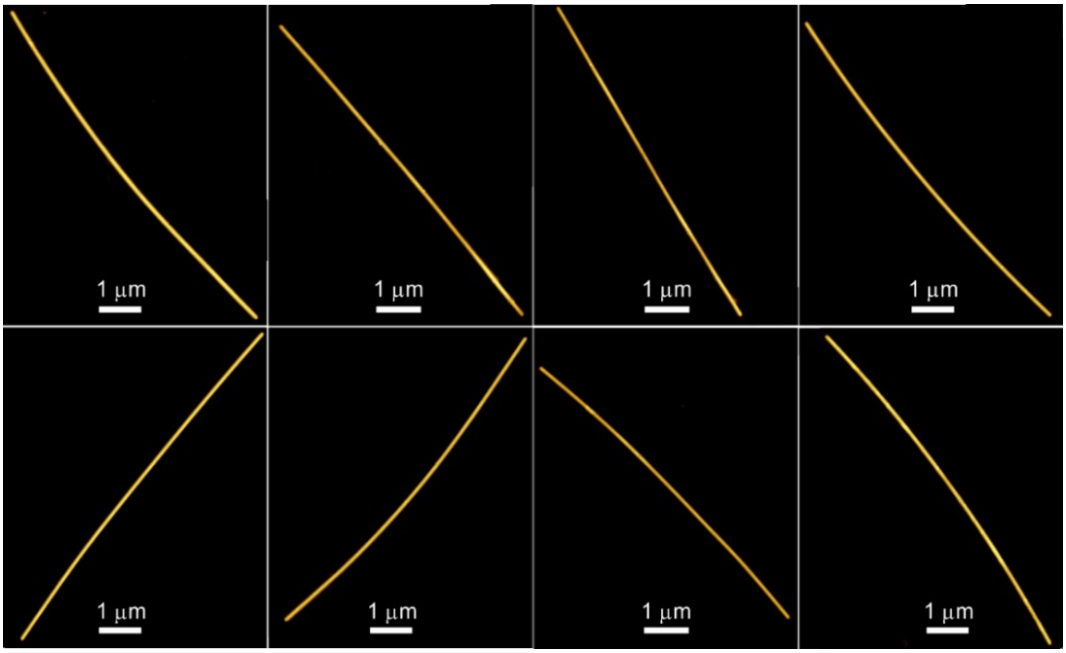

Fig. S12 Representative AFM images of Ag NWs in different positions.

Section 8.1 FDTD simulation for AFM-Au tip enhanced Raman spectra

Considering the difference between Au tip with radius of curvature and single Au NPs, the AFM-correlated $|E/E_0|$ distributions was calculated using a 3D-FDTD simulation with an enhancement of 1.4×10^7 and 5.5×10^7 for the Au tip with radius of curvature of 15 nm and 50 nm. Based on above analysis, this single hot spot structure has several advantages compared with the tip-enhanced technique: (i) a single hot spot structure can be fabricated with a facile approach and well-defined nanostructure, which provides a giant E-field enhancement; (ii) the single hot spot structure can be conveniently located using Raman optical microscopy, which brings reproducible SERS features; and (iii) this single hot spot can overcome the TERS limitation and be extended to practical applications. Therefore, this single hot spot structure reproducibly and sensitively offers a robust platform for SERS study.

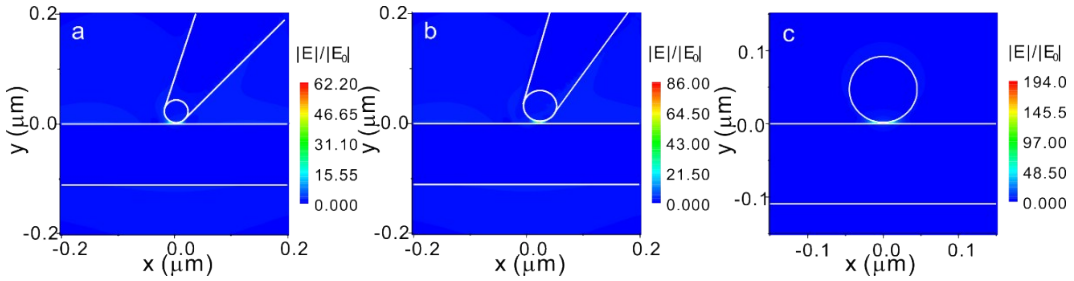

Fig. S13 Comparison of the respective 3D-FDTD calculations with 633 nm laser for the Au tip with radius of curvature of 15 nm (a) and 50 nm (b) reported in the literature as well as the single Au NP (c) on the surface of the

Ag NW, where the incident light is injected along the z-axis with an electric field along the y-axis.

Section 9. Supplementary applications of a single hot spot platform

Section 9.1 The experimental measurement for dual analytes

Samples for dual-analyte SERS measurement were created by mixing equimolar amounts of MG (25 fmol = 5 μL × 5 nM, 2.5 fmol = 5 μL × 0.5 nM, 0.25 fmol = 5 μL × 0.05 nM) and R6G (25 fmol = 5 μL × 5 nM, 2.5 fmol = 5 μL × 0.5 nM, 0.25 fmol = 5 μL × 0.05 nM) with 1 mL of Ag NWs (200-fold diluted), providing 50, 5 and 0.5 fmol analytes for detection. As 1μL of the above mixture was dropped onto the Si wafer and then left to dry, a drop of diluted Au NPs were added onto the above Si wafer to assemble the single hot spot structure. Thus, there are an average of 122 (12.2, 1.22) molecules of MG and 122 (12.2, 1.22) molecules of R6G within the efficient area (2500 nm^2) between the Au NP and Ag NW when varying the analyte MG or R6G concentration from 25, 2.5 to 0.25 fmol.

Section 9.2 The SERS mapping for dual-analyte with different numbers of molecules

In general, most dual-analyte detection is carried out on liquid colloidal particles, so it is possible that two or more molecules could compete for the same hot spot on the NP surface. Alternatively, more molecules could act independently at the two different hot spots within a diffraction-limited spot; consequently, the degree of spectral wandering[9, 10] is measured with a change of 7 cm^{-1}. In this report, the dual-analyte detection was carried out on a dry SERS substrate; thus, the degree of the spectral wandering is considerably weaker.

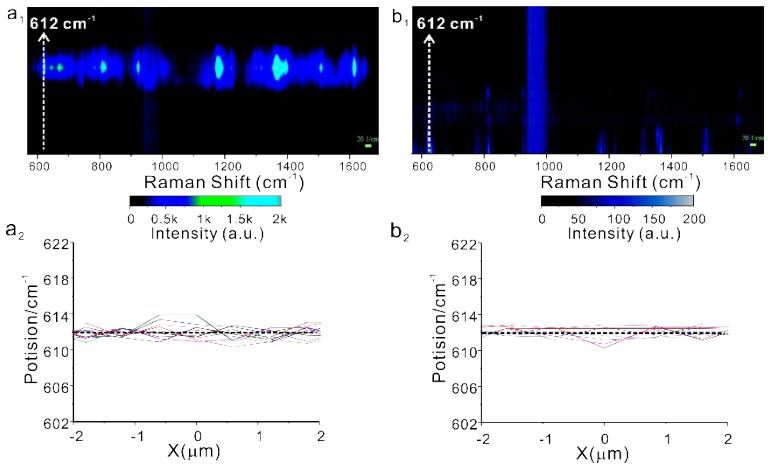

Fig. S14 (a_1 and b_1) Corresponding spatial serials SERS signals of MG and R6G bound in the hot spot area with different concentration (0.5 nM and 0.005 nM) with false color representing the signal intensity (blue/green is highest, black is lowest); (a_2 and b_2) the fluctuation of the band at 612 cm^{-1} (R6G) under different concentrations (0.5 nM and 0.005 nM) for dual-analyte detection.

Section 10. Supplementary mechanism of capturing molecules for single hot spot platform

Section 10.1 Analyte preparation for versatility detection

For the formation of a single hot spot site, 1 μL of Ag NWs (1.9×10^5/μL) diluted with water was dropped onto the Si wafer. Subsequently, after drying, 1 μL of diluted Au NPs (1.5×10^6/μL) was added onto the above Si wafer. As the single hot spot structure was formed, a drop of aqueous analyte (1 μL), such as cysteine, adenosine-5'-triphosphate, methamphetamine and paraoxon with different concentrations was placed onto the Si wafer and then examined with SERS.

Section 10.2 The "nano-channel" of hot spot structure for trapping molecules

Capillary action is an important transport mechanism in nano-fluidics. The fundamentals of the current understanding of capillary action are based on the early 19th century contributions made by Young and Laplace. The Young-Laplace theory of capillarity relates the pressure difference across a curved interface (Laplace pressure) to the surface tension acting on the interface as a result of its curvature. For water at room temperature, if a channel height is 108 nm with a contact angle of 18º, the capillary pressure P_{cap} is 13 bar.[11] For an ambient pressure P_0 of 1 bar, this implies that the liquid meniscus is at a pressure of -12 bar. In other words, the capillary-induced negative pressure at the liquid meniscus will increase as the channel height increases; therefore, in this report, the "nano-channel" formed between the Ag NW and Au NP will efficiently capture the target analyte solution because larger negative pressure appears within the hot spot than that of the channel formed between the Ag NW and Si wafer.

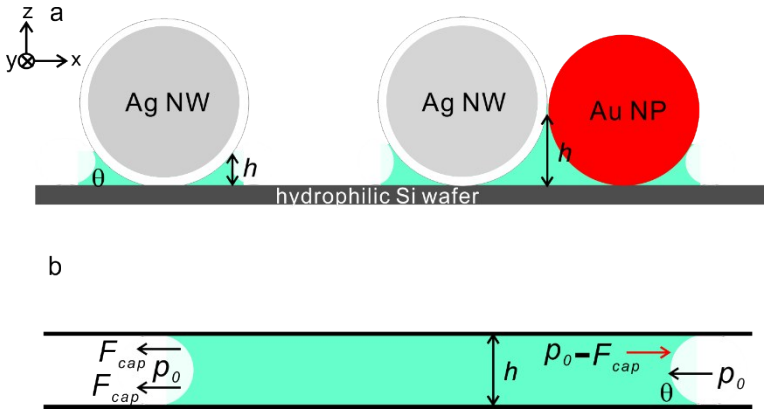

Fig. S15 (a) Schematic diagram of the formation of the nano-channel and (b) the calculation of the capillary-induced negative pressure around the Ag NW and single hot site area.

References

1. Y. G. Sun, B. Gates, B. Mayers and Y. N. Xia, *Nano Lett*, 2002, **2**, 165.

2. J. H. G. K. Liu, P. C. Zheng, G. L. Shen, J. H. Jiang, R. Q. Yu,Y. Cui and B.Ren, *J. Phys. Chem. C*, 2010, **112**, 6499.
3. U. Hartmann, *Ultramicroscopy*, 1992, **42**, 59.
4. N. Mitarai and F. Nori, *Adv Phys*, 2006, **55**, 1.
5. H. Wei, F. Hao, Y. Z. Huang, W. Z. Wang, P. Nordlander and H. X. Xu, *Nano Lett*, 2008, **8**, 2497.
6. A. W. Sanders, D. A. Routenberg, B. J. Wiley, Y. N. Xia, E. R. Dufresne and M. A. Reed, *Nano Lett*, 2006, **6**, 1822.
7. H. X. Xu, E. J. Bjerneld, J. Aizpurua, P. Apell, L. Gunnarsson, S. Petronis, B. Kasemo, C. Larsson, F. Hook and M. Kall, *Nanoparticles and Nanostructured Surfaces: Novel Reporters with Biological Applications*, 2001, **2**, 35.
8. M. W. Knight, N. K. Grady, R. Bardhan, F. Hao, P. Nordlander and N. J. Halas, *Nano Lett*, 2007, **7**, 2346.
9. S. L. Kleinman, E. Ringe, N. Valley, K. L. Wustholz, E. Phillips, K. A. Scheidt, G. C. Schatz and R. P. Van Duyne, *J. Am. Chem. Soc.*, 2011, **133**, 4115.
10. E. C. Le Ru, P. G. Etchegoin and M. Meyer, *Journal of Chemical Physics*, 2006, **125**, 204701.
11. N. R. Tas, P. Mela, T. Kramer, J. W. Berenschot and A. van den Berg, *Nano Lett*, 2003, **3**, 1537.